A Pulsed Source for Kr(5s[3/2]$_1$) Resonance State Atoms Using Two-Photon-Driven Amplified Spontaneous Emission: Measurement of Quenching Rate Constants

V. A. Alekseev[†] **and D. W. Setser***

Department of Chemistry, Kansas State University, Manhattan, Kansas 66506

Received: January 7, 1999; In Final Form: March 30, 1999

Krypton resonance state atoms, Kr(5s[3/2]$_1$), were generated in a static cell by two-photon laser excitation of the Kr(5p[5/2]$_2$) state with amplified spontaneous emission (ASE) at 877.7 and 810.4 nm in a few Torr of Kr gas. The 877.7 nm transition, which terminates on the resonance state, constitutes ≥90% of the ASE intensity. The vacuum ultraviolet emission at 123.6 nm was used to monitor the Kr(5s[3/2]$_1$) concentration, which decayed with an effective lifetime of 2 μs in the absence of added reagents. Total quenching rate constants at 300 K for the resonance state atoms were measured for 30 molecules by observing the decay rates of the Kr(5s[3/2]$_1$) atoms as a function of added reagent gas. The rate constants (cm^3 molecule^{-1} s^{-1}) range from 1.4×10^{-11} for N_2 and 0.60×10^{-11} for CF_4 to $(80-90) \times 10^{-11}$ for hydrocarbons. Rate constants for most polyatomic molecules exceed 30×10^{-11} cm^3 molecule^{-1} s^{-1}. Comparison to the quenching rate constants of the Kr(5s[3/2]$_2$) metastable atoms shows that the rate constants of the resonance states are ∼35% larger for reagents with quenching cross sections larger than 20 Å^2. For a set of 11 reagents, comparison also is made with the rate constants for the (6s) and (6s′) resonance states and the (6p) states of Xe; the latter have nearly the same energy as the Kr(5s) resonance state.

Introduction

In a recent paper[1] we described two-photon, pulsed laser excitation to the Xe(6p,6p′,7p) states in a few Torr of Xe under conditions such that amplified spontaneous emission (ASE) generated useful concentrations of the Xe(6s[3/2]$_1$) and Xe(6s′[1/2]$_1$) resonance state atoms for subsequent kinetic studies. Since the resonance state atoms are produced by the ASE pulse, which occurs within the laser pulse, the preparation time is very short. Although the nonlinear phenomena responsible for generation of the lower energy states is complex,[2−5] the two-photon laser driven ASE method was shown to be a convenient time-resolved laboratory source for the two resonance state Xe atoms.[1] The vacuum ultraviolet emission at 147 and 129 nm was used to monitor the decay rates of these Xe(6s[3/2]$_1$) and Xe(6s′[1/2]$_1$) atoms, and the method was used to measure the total quenching rate constants for added reagent gases. Due to the strong fluorescence signal, the quenching rate constants measured with this method had an uncertainty of less than 5%. The ASE method also could be used to generate the Xe(6s[3/2]$_2$) and Xe(6s′[3/2]$_0$) metastable state atoms, but an additional monitoring technique would have to be added to the experiment to follow their concentrations. The discharge flow-reactor method is a more convenient way of studying metastable rare gas atoms at low pressure.[6] The two-photon excitation method also can be used to prepare and study the reactions of individual Xe(6p,6p′,7p) states;[7] however, care must be exercised to avoid complications arising from the ASE phenomena.[2]

In the present work, we have extended the two-photon laser driven ASE method to produce Kr(5s[3/2]$_1$) resonance state atoms, 10.03 eV, via laser excitation of the Kr(5p[5/2]$_2$) state. The required laser wavelength is 216.7 nm, which can be routinely obtained using a BBO-II doubling crystal. After demonstration of the time-resolved method for generating the Kr(5s[1/2]$_1$) resonance atoms, the method was used to measure rate constants for 30 reagents that were selected to represent molecules with a broad range of properties. These rate constants (or thermal averaged cross sections) are compared to those of the Kr(5s[3/2]$_2$) 9.92 eV metastable state.[6,8] Except for N_2, CO, H_2, and CF_4, the quenching cross sections of molecules for the resonance state are somewhat larger than for the metastable state. The products from reactions of the metastable and resonance states of Kr with many of the reagents have already been discussed;[6,9] however, we were able to observe CO(A$^1\Pi$) formation from Kr(5s[3/2]$_1$) reacting with ^{12}CO and ^{13}CO. The rate constants for the Kr(6s[3/2]$_{2,1}$) atoms also are compared to the rate constants[7a] of Xe(6p[3/2]$_2$) atoms, which have an energy of 9.82 eV. During the course of the present work, we also measured a few more rate constants for the two Xe resonance states that were studied in our previous work.[1] An effective database now exists that permits the rate constants for the lowest energy metastable and resonance states of Ar, Kr, and Xe to be compared.[1,6,8−12] These quenching cross sections are used to discuss the dipole−dipole quenching model, as well as other long-range quenching models.

Experimental Methods

The experiments were performed in a stainless steel cell with 25 cm long laser baffle arms. The cell, which was attached to the entrance flange of a monochromator, had a LiF window for observation of the vacuum ultraviolet (vacuum UV) emission. The laser beam, which passed vertically through the cell, was parallel to the entrance slit of the monochromator. A diagram of the experimental apparatus was shown in Figure 2 of ref 1. The output from a Lambda Physik dye laser (LPD 3002) pumped with a XeCl laser (Questek 2840) was doubled with BBO-II crystal to obtain the tunable ultraviolet laser pulses. Stilbene 420 dye was used to obtain the 216.7 nm wavelength

[†] Permanent address: Photonics Department, Institute of Physics, St. Petersburg University, 198904 St. Petersburg, Russia.

10.1021/jp990105s CCC: $18.00
Published on Web 05/05/1999

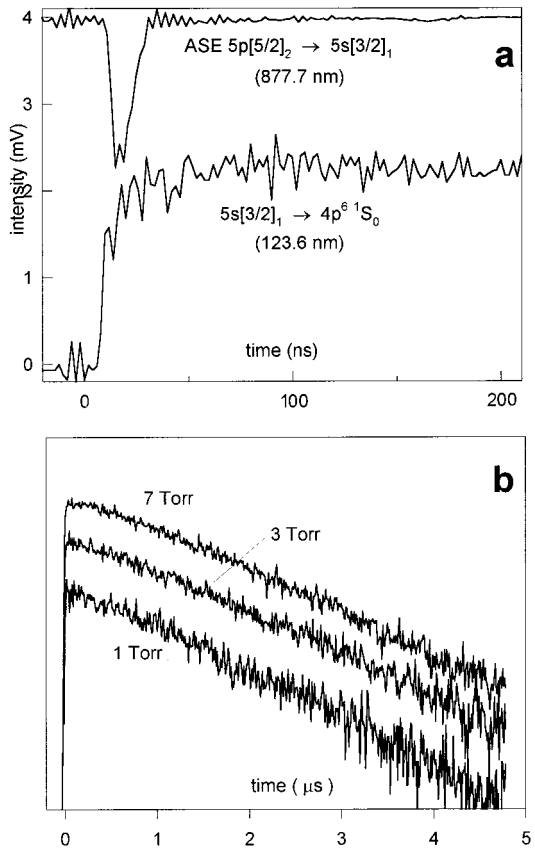

Figure 1. (a) Waveforms of the ASE emission and the 123.6 nm resonance emission for two-photon excitation of the Kr(5p[5/2]$_2$) state with focused laser pulse energy of ~1 mJ in 2 Torr of Kr. (b)Waveforms of the 123.6 nm resonance emission (log scale) for different Kr pressures.

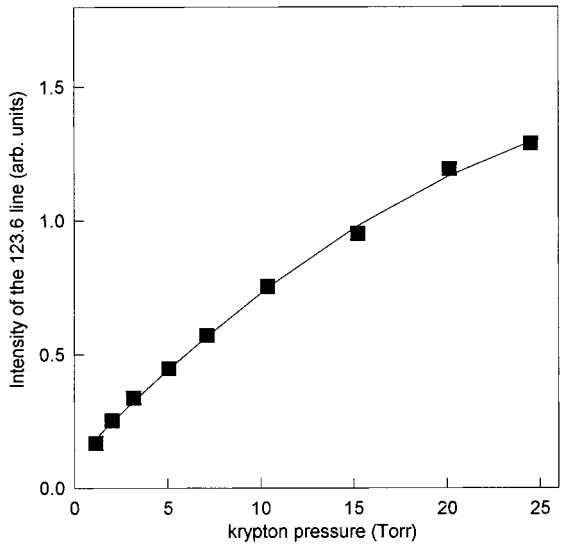

Figure 2. Intensity of the 123.6 nm resonance emission vs Kr pressure.

that was required for two-photon excitation to the Kr(5p[5/2]$_2$) state. The laser pulse had a full width at half-maximum of ~15 ns and the energy was 0.05−0.2 mJ per pulse, as measured with a Precision power meter (model RJP-735). The dye laser was operated without an Etalon and the bandwidth was 22 GHz for the doubled wavelength. Most experiments were done with mildly focused conditions using a 50 cm focal length lens (just as for the ASE generation of the Xe resonance states).[1]

The vacuum UV monochromator (0.25 m Acton Research) was equipped with a 1200 grooves/mm concave grating blazed at 120 nm and a Hamamatsu R 1259 solar-blind photomultiplier tube (PMT), which has maximum sensitivity at ~120 nm, but the range extends from 115 to 190 nm. This monochromator has only one reflective surface and the 123.6 nm Kr resonance emission could be easily observed. The output signal of the PMT was digitized (Hewlett-Packard 54510 digital storage oscilloscope) and transferred to a computer for storage and analysis. The monochromator was evacuated to less than 10^{-4} Torr using a mechanical pump in combination with a small oil-diffusion pump. The pumping system was separated from the monochromator with a liquid-N_2 trap. This monochromator and PMT had excellent capability for monitoring the Kr and Xe resonance emission lines in the vacuum UV without concern for the scattered laser light; however, it was less useful in searches for emission spectra from product states because of its inability to observe emission for $\lambda > 190$ nm.

The ASE lines at 877.7 and 810.4 nm from the Kr(5p[5/2]$_2$) atoms were observed in the forward direction, relative to the laser beam, with a 0.5 m Minuteman monochromator equipped with grating blazed at 500 nm and a Hamamatsu R-955 PMT. After passing through the cell, the laser beam and associated ASE light were directed to the entrance slit of this monochromator; a filter was used to cut the UV laser light. The intensities of the ASE lines were strong, and a diffuser (an etched quartz plate) was placed in front of the entrance slit to fill the monochromator optics with light and to avoid damage to the PMT. The difference in response at 877.7 vs 810.4 nm is, at least, an order of magnitude in favor of 810.4 nm, as measured by comparison of these intensities from a low-pressure Kr discharge lamp and the predicted intensities from the Einstein coefficients.

Experiments were done at room temperature using Kr pressures of 1−10 Torr plus added reagent gases. The Kr was obtained from Spectral Gases, and the reagent gases were obtained mainly from Matheson. Whenever possible, the reagents were condensed and degassed before loading into the cell. The reagent and Kr pressures were measured with a 0−10 Torr pressure transducer (MKS Baratron). The experiments to measure rate constants consist of recording the first-order decay profiles of the Kr(5s[3/2]$_1$−^{1}S$_0$) resonance emission at 123.6 nm for constant Kr pressure with variable added reagent gas pressures. The decay profiles were recorded without a preamplifier using the digital oscilloscope.

Experimental Results

A. Generation of Kr(5s[3/2]$_1$) Atoms by Two-Photon Excitation of Kr(5p[5/2]$_2$). Most experiments were performed with a mildly focused laser beam in a few Torr of Kr. The ASE emission in the forward direction was monitored at the wavelengths of the Kr(5p[5/2]$_2$−5s[3/2/]$_2$) and Kr(5p[5/2]$_2$−5s[3/2]$_1$) transitions at 810.4 and 877.7 nm, respectively. The observed intensity ratio of these ASE transitions in the forward direction was 1.0 ± 0.2 for most experimental conditions. The ASE transitions had the same time profiles as the laser pulse. No ASE emission was observed from the Kr(5p[5/2]$_3$) state, which lies only 13 cm^{-1} below the (5p[5/2]$_2$) level. Thus, collisions of the laser prepared (5p[5/2]$_2$) state with Kr atoms at pressures ≤10 Torr do not couple the (5p[5/2]$_3$) and (5p[5/2]$_2$) states during the laser pulse. As discussed in the Experimental Section, calibration of the monochromator's wavelength response function with a Kr lamp showed that the detection system was ≥10 times more sensitive at 810.4 nm. Thus, the relative ASE intensities measured in the forward direction suggest that the stimulated emission method produces a higher

(factor of 10) concentration of Kr(5s[3/2]$_1$) atoms than Kr(5s[3/2]$_2$) atoms. This actually is expected because the Einstein coefficients[13] for the 877.7 nm transition to Kr(5s[3/2]$_1$) is 2.6 $\times$ 10^7 s^{-1}, whereas that to the metastable Kr(5s[3/2]$_2$) state at 810.4 nm is 1.1 $\times$ 10^7 s^{-1}. It must be remembered that the forward emission could be a mixture of the ASE plus stimulated electronic Raman scattering (SERS);[1] thus, the forward intensities are only suggestive of the relative concentrations of the resonance and metastable states. We were mainly interested in obtaining the 123.6 nm resonance emission with sufficient intensity so that the Kr(5s[3/2]$_1$) state could be studied. Therefore, we did not characterize the ASE phenomena in Kr in any further detail.

The rise time of the 123.6 nm fluorescence signal was within the duration of the ASE pulse (see Figure 1a). After termination of the ASE pulse, the 123.6 nm fluorescence exhibits single-exponential decay (see Figure 1b) with a decay time of $\sim$2 μs. We found no evidence for any significant formation of Kr(5s[3/2]$_1$) atoms after the laser pulse terminated, and the population remaining in the laser pumped Kr(5s) level seems to be minimal. The 123.6 nm fluorescence intensity scales linearly with the Kr pressure as shown by the plot of the maximum (zero time) observed intensity vs Kr pressure in Figure 2. The 123.6 nm fluorescence intensity also seemed to scale with the square of the laser energy, as expected. For Kr pressures of a few Torr and laser energy $\sim$0.1 mJ, the intensity of the 123.6 nm signal was strong and $\sim$1000 laser shots gave a satisfactory waveform to monitor the decay of the (5s[3/2]$_1$) atom concentration. Because of the difficulty of obtaining shorter laser wavelengths, we made no effort to utilize the two-photon excitation of the higher energy Kr(5p[3/2]$_2$ and 5p[1/2]$_0$]) states for generation of the Kr(5s[3/2]$_1$) atoms. In principle, the 5p[1/2]$_0$ level offers the advantage that *only* the Kr(5s[3/2]$_1$) state would be generated by the ASE pulse. For identification of products from quenching of the Kr(5s) resonance state, this pumping scheme could have some advantages.

Although the natural radiative lifetime of Kr(5s[3/2]$_1$) atoms is 3.2$-$4.5 ns,[13a,14] the effective lifetime of the resonance radiation in pure Kr is lengthened greatly due to radiation trapping.[15,16] The effective lifetime, τ_{eff}, depends on Kr pressure and other experimental factors, such as the distance between the observation window and the laser beam (i.e., the volume containing the excited atoms) and the cell dimensions. For Kr pressures of 1$-$10 Torr and a distance of 2$-$3 mm, τ_{eff} was a few microseconds. In this pressure range, the decay rate of the 123.6 nm emission depends only weakly on Kr pressure; see Figure 1b. The Holstein theory[15] and more recently developed models[16a] for the transport of resonance radiation predict a time region in which the exponential decay rate is independent of pressure with a decay constant given by

$$\beta_0 = \frac{0.269}{\tau_0}\left(\frac{\lambda}{R}\right)^{1/2} \qquad (1)$$

where R is a geometrical factor (distance between the laser beam and observation window) and τ_0 is the natural lifetime of the transition having wavelength λ. Equation 1 gives $\beta_0 \sim$ (0.5$-$1.0) $\times$ 10^6 s^{-1} for $R \sim$ 3 mm, which is in acceptable agreement with our data (Figure 1b). Equation 1 only is valid if the resonance state is not quenched by collisions with the parent gas, and we can conclude that quenching of Kr(5s[3/2]$_1$) is negligible, relative to radiative decay, up to 20 Torr of Kr. This conclusion is in accord with rate constant values assigned to two- and three-body quenching processes of Kr(5s[3/2]$_1$) atoms.[6b,17]

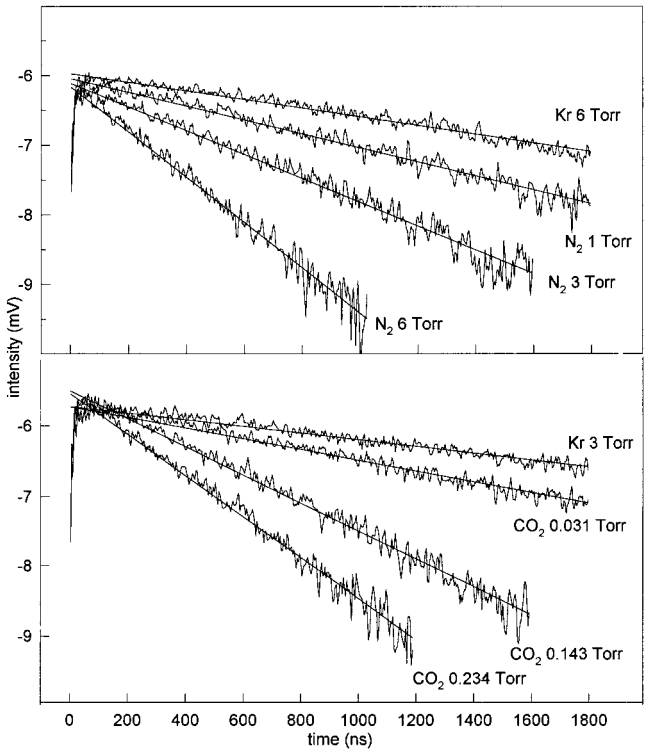

Figure 3. Waveforms of the 123.6 nm resonance emission intensity (log scale) used to measure the quenching rate constants by N_2 (upper panel) and CO_2 (lower panel). The Kr pressures in the experiments were 6 and 3 Torr, respectively.

The geometrical arrangement of the cell can affect the decay time for the resonance radiation. In particular, if the diffusion of resonance radiation affects the field of view, the decay may be nonexponential.[16b] We always observed single-exponential decay in our experiments, if the laser beam passed in front of the entrance slit of the monochromator. The explanation is that after a time such that the radiation has reached the observation window, the concentration of excited atoms in each element of volume can be factored, as shown in eq 2, into a radial dependence and a time dependence.

$$N(r,t) = f(r)\exp(-\beta t) \qquad (2)$$

The decay constant, β, includes all processes in the observed volume that deplete the excited atoms. When a reagent gas is added, $\beta = \beta_0 + k_Q[Q]$, where the first term is determined by (1) for our pressure range. Measurement of β for a range of [Q] provides a good way to obtain k_Q. For more details about the radiation imprisonment problem, see refs 15 and 16 and references therein. A set of waveforms obtained for mixtures with N_2 is shown in Figure 3 as an example of the quenching data. Adding a few Torr of N_2 reduces the decay time of the 123.6 nm fluorescence, but the N_2 concentration does not affect the peak intensity of the signal, i.e., the Kr(5s[3/2]$_1$) formation step via the ASE is not affected by the added N_2. We did not study the temporal behavior of the 123.6 nm emission for different alignments of laser beam relative to the entrance slit in any detail. However, such experiments were done for Xe(6s[3/2]$_1$) previously,[1] and these geometrical factors were found not to affect the quenching rate constant measurements.

In the present work, our objective was to develop the ASE method for generation of the Kr(5s[3/2]$_1$) state atoms for kinetic studies. Two-photon excitation of the $J = 0$ and 2 levels in the Kr(5p) manifold without ASE could be the desired goal for direct studies of these states. We observed that laser pulses of

reduced energy or more gentle focusing eliminated the ASE signal from the $Kr(5s[3/2]_2 \rightarrow 5s[1/2]_{1,2})$ transitions. In fact, elimination of the ASE following two-photon excitation of Kr(5p) atoms seems to be much easier than for excitation of Xe(6p, 6p′, 7p) states in the same cell.[2] Thus, systematic study of the quenching reactions of the Kr(5p) states can be done rather easily using the two-photon excitation method, if that is the desired objective. Our laboratory has done one such experiment to measure the reaction rate constant of $Kr(5p[5/2]_2)$ with F_2.[18] In this context, the recent two-photon excitation experiments to measure the quenching rate constants of the Ar(4p) states should be noted.[19]

B. Quenching Constants for $Kr(5s[3/2]_1)$ Atoms. Quenching rate constants of the Kr resonance state atoms were measured for 30 reagent molecules using a Kr pressure of 2−5 Torr and laser energy of ∼0.1 mJ. Single-exponential decay could be observed over two decades of $Kr(6s[3/2]_1)$ atom concentration. A set of waveforms was already shown in Figure 3 (upper panel) to illustrate the first-order decay of the $Kr(6s[3/2]_1)$ atom concentration in N_2. In extracting decay constants, care must be exercised because the decay rates can change by an order of magnitude as the reagent is added, and the waveforms were acquired without a preamplifier to avoid distortion. Also, one must guard against after-pulses of current from the PMT, if the signal is too strong. The time profiles are shown in Figure 3 (lower panel) for the decay of the resonance atom concentration in CO_2 in order to display an example with a large quenching rate. The quenching data were taken by first adding Kr to the cell and subsequently adding the reagent from a reservoir via a needle value. The increase in pressure was measured by a pressure transducer placed directly on the cell. A waveform was taken for each reagent pressure after sufficient time had elapsed for mixing. In measuring the decay times, the reagent pressure usually was increased until the decay rates increased by a factor of 8−10. The Stern−Volmer plots for several molecules are shown in Figure 4; the data for the other reactions are of similar quality. Except for Xe, CF_4, H_2, CO, and N_2, the quenching rates are very fast, and <0.5 Torr of the reagent was sufficient to establish the Stern−Volmer plots. The 300 K rate constants for the $Kr(5s[3/2]_1)$ atoms are listed in the first column of Table 1. Experiments were done with ^{13}CO and D_2 vs ^{12}CO and H_2 to serve as specific tests for the dipole−dipole model of quenching. The rate constants in Table 1 show that isotopic substitution had no appreciable effect on the magnitude of the total quenching rate constants of $Kr(5s[3/2]_1)$ atoms.

The typical uncertainty in the k_Q values for different data sets was ±5%. A specific test for reproducibility was made for Xe and CO as a reagent. Three independent measurements of k_Q were made in the first series of experiments. Six months later, two more independent data sets were acquired. The rate constants are (2.9 ± 0.1) and (3.0 ± 0.3) × 10^{-11} cm^3 s^{-1} for Xe and (4.9 ± 0.1) and (4.8 ± 0.1) × 10^{-11} cm^3 s^{-1} for CO. The ASE method for generating Kr (and Xe) resonance state atoms provides a very reliable way to measure total quenching constants. The measurement of the partial pressures of the reagents is the limiting factor to the reliability of the rate constants.

C. Products from Quenching of $Kr(5s[3/2]_1)$ Atoms. Given the ≤200 nm limitation of the wavelength range of the solar-blind PMT, identification of possible products were attempted only for CO, Xe, and H_2. The $CO(A^1\Pi-X^1\Sigma^+)$ emission was easily observed from the $Kr(5s[3/2]_1)$ + ^{12}CO and ^{13}CO reactions, and CO(A) is a major product; see Figure 5a. Yu and Wang have reported that $CO(d^3\Delta$ and $a'^3\Sigma^+)$ also are

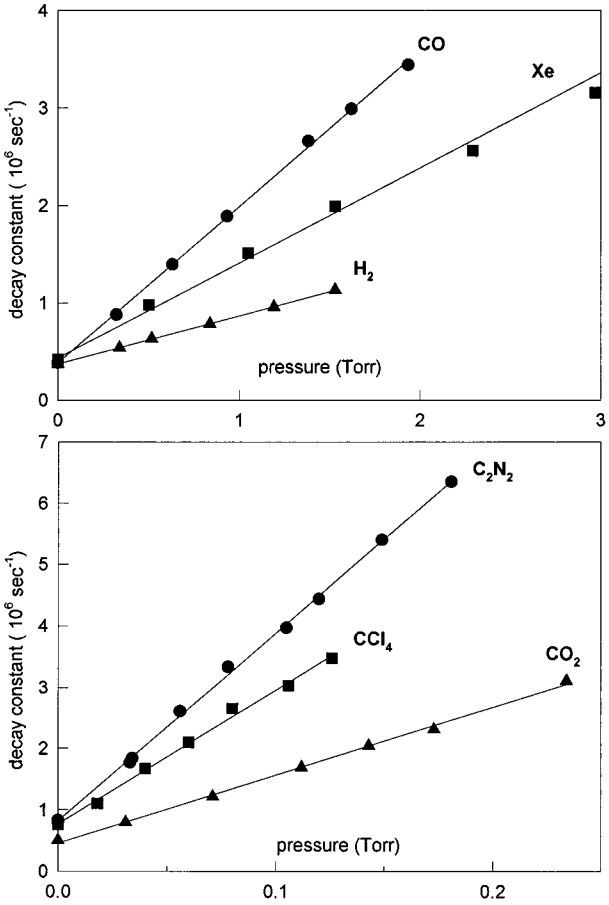

Figure 4. Decay constants of 123.6 nm emission from 2 Torr of Kr vs pressure of different reagents. Note that the effective lifetime of 123.6 nm emission with no reagent added to the cell is not a constant and depends on the distance between the laser beam and the observation window. This distance was constant for each set of experiments with a given reagent gas, but not from one day to another.

primary products.[20] These same excited CO states also are products from the reaction of the metastable $Kr(5s[3/2]_2)$ atoms with CO.[21] However, the Kr resonance state concentration should greatly exceed the Kr metastable state concentration in our experiment. The source for CO(A) formation was confirmed to be the resonance atoms by noting that the CO(A) emission time profiles exactly matched those for $Kr(5s[3/2]_1)$. The $^{13}CO(A-X)$ emission spectrum differs only slightly from that of $^{12}CO(A-X)$, and this difference seems to be a consequence of the altered vibrational level spacing of the two molecules for high v' levels, rather than from any change in quenching mechanism. The CO(A−X) emission spectra from the $Kr(5s[3/2]_2)$ reaction with ^{12}CO and ^{13}CO obtained at higher resolution shown in ref 21 verifies this claim. Each reaction gives nearly the same CO(A−X) emission intensity, even though only $^{13}CO(v'=13)$ has rotational transitions in resonance (ΔE = 8 cm^{-1}) with the $Kr(5s[3/2]_1)$ atom energy.[22] The $CO(A^1\Pi)$ radiative lifetime is sufficiently short that collisional quenching or vibrational relaxation is not important, and we conclude that the main quenching process of Kr(5s) resonance atoms proceeds by the same mechanism for both ^{12}CO and ^{13}CO. Our conclusion thus differs from the early study by Vikis[22] who reported fluorescence from resonance excitation of $^{13}CO(A,v'=13)$, but not $^{12}CO(A,v'=12)$ from observations in the 200−320 nm region. However, the strong vacuum ultraviolet emission shown in Figure 5a clearly shows that $^{12}CO(A)$ is a major product from ^{12}CO + $Kr(5s[3/2]_1)$. The collisional transfer of $CO(d^3\Delta$ and $a'^3\Sigma^+)$ molecules to CO(A) can be a contributing, but not the

TABLE 1: Quenching Rate Constants for Kr(5s[3/2]$_1$) with Comparison to Kr(5s[3/2]$_2$ and Xe(6p[3/2]$_2$) Atoms

	rate constant, 10^{-11} cm^3 molecule^{-1} s^{-1}			
reagent	Kr(5s[3/2]$_1$)[a]	Kr(5s[3/2]$_2$)[b]		Xe(6p[3/2]$_2$)[c]
Xe	2.9 (8.2),[d] 3.0[a]	16 (46)[d]	18.0 ± 1.0	8.7
H_2	1.6 (0.9)	3.0 (1.7)	3.7 ± 0.3	78
D_2	1.4 (1.1)	2.5 (1.9)		
N_2	1.4 (2.6)	0.39 (0.7)	0.41 ± 0.02	36
^{12}CO	4.9 (8.8), 4.8[a]	5.8 (10.5)	5.7 ± 0.2	74
^{13}CO	4.5 (8.4)		4.5 ± 0.5	
O_2	26 (50)	16 (31)	(37)[e]	78
NO	24 (45)	19 (35)		74
CO_2	34 (75)	40 (85)		
OCS	53 (126)			86
N_2O	43 (93)	31 (66)		75
NO_2	56 (123)			112
SO_2	74 (159)	58 (139)		
CF_4	0.66 (1.7)	0.07 (0.17)	0.079 ± 0.008	30
CH_4	75 (110)	37 (54)	32.0 ± 1.5	
CF_3Cl	40 (110)	14 (34)		112
CF_3Br	56 (164)	50 (145)		
CH_3F	48 (94)	46 (90)		
CH_3Cl	52 (116)			
$CHFCl_2$	63 (172)		≈29[f]	78
CCl_4	68 (200)	69 (201)	46 ± 4	62
SF_6	33 (97)	18 (53)		
C_2H_4	78 (144)			
C_2H_2	46 (82)			
C_2N_2	94 (214)	51 (114)		
C_2H_6	82 (154)	50 (93)		
$CH_3CH{=}CH_2$	81 (172)			
cyclo-C_3H_6	69 (147)			
C_3H_8	74 (160)			
C_4H_{10}	81 (191)			
C_5H_{12} (neopentane)	85 (204)	72 (169)		

[a] Measured in this work; the least-square uncertainties in the slopes of the Stern−Volmer plots were ≤5%. The double entries for Xe and CO are independent sets of measurements separated by 6 months in time. The Xe quenching constants for Kr(5s′[1/2]$_1$[17b] and 5s′[1/2]$_0$)[6b] are 0.37×10^{-11} and 24.4×10^{-11} cm^3 s^{-1}, respectively. [b] Taken from refs 6 and 8. The uncertainties given for the most recent work is representative of the uncertainty for rate constants measured in flow reactors. [c] Taken from ref 7a; the energy of Xe(6p[3/2]$_2$) is 9.82 eV; the entry for SO_2 is for the Xe(6p[1/2]$_0$) state. [d] The numbers in parentheses are the thermal reaction cross sections, $\sigma_Q = k_Q/\langle v \rangle$, in units of Å^2. [e] This is a true cross section measurement for the 575−810 m/s velocity range; ref 24. [f] This entry actually is for CHF_2Cl; the value for $CHFCl_2$ should be equal to, or larger, than this value.

major, factor to the total CO(A−X) emission; more detail about the collisional relaxation of CO(d,a′) molecules is given in ref 21.

No product emission was observed from the reaction with either H_2 or D_2, and we can conclude that KrH* (KrD*) is not a product. The only remaining alternative is excitation transfer to the repulsive $H_2(a^3\Sigma^+)$ state. The reaction of metastable Kr(5s[3/2]$_2$) atoms with N_2 gives mainly N_2 triplet state products (the $B^3\Pi_g - A^3\Sigma^+_u$ bands are easily observed) and perhaps some N atoms.[17c,23] We did not examine the emissions from the Kr(5s[3/2]$_1$) + N_2 reaction; however, Yu et al. did not observe any N_2* emission from the vac. UV to the visible range in this work.[20] The quenching rate constant by N_2 for the resonance state is ∼3.6 times larger than for the metastable state; the latter gives $N_2(B^3\Pi_g)$ as the main product.[23] On the other hand, the quenching constant for the second metastable state is 6 times smaller than for the first metastable state; these experiments, which were done in a flow reactor,[6b] failed to identify any product from the Kr(5s′[1/2]$_0$) reaction. Identification of the specific N_2 product states is required in order to understand the rather extreme variation of rate constants for quenching of the Kr(5s, 5s′) states by N_2.

The reaction of Kr(5s[3/2]$_1$) atoms with Xe gives Xe(6s[3/2]$_1$) emission at 147 nm, as shown in Figure 5b. The resonance emission at 125 and 129 nm from Xe(5d[1/2]$_1$) and Xe(6s′[1/2]$_1$) atoms, respectively, were not observed for Xe pressure of 1−6 Torr. Similar observations were made by Cook and Leichner[17b] in e-beam excitation studies of Kr with added Xe impurity. The mechanism for quenching by Xe seems to be transfer of energy from the Kr(5s[3/2]$_1$) state into states in the Xe(5d or possibly 6p) manifold. Based upon energy defect arguments, the expected primary products would be the Xe(5d[7/2]$_3$, [3/2]$_2$, [7/2]$_4$) states rather than Xe(5d[1/2]$_1$ or [1/2]$_0$]); the latter are 930 and 1145 cm^{-1} below the Kr(5s[3/2]$_1$) state, respectively.

$$\begin{aligned} \mathrm{Kr(5s[3/2]_1) + Xe} &\rightarrow \mathrm{Xe(5d[7/2]_3) + Kr} - 54\ \mathrm{cm^{-1}} \\ &\rightarrow \mathrm{Xe(5d[3/2]_2) + Kr} + 584\ \mathrm{cm^{-1}} \\ &\rightarrow \mathrm{Xe(5d[7/2]_4) + Kr} + 720\ \mathrm{cm^{-1}} \end{aligned} \quad (3)$$

The highest member of the Xe(6p) manifold, 6p[1/2]$_0$, is 788 cm^{-1} below the Kr(5s[3/2]$_1$) state. At the Xe and Kr pressures of this experiment, quenching of the Xe(6p) intermediate levels is minor and the Xe(6p) states will radiatively decay to the Xe(6s[3/2]$_{2,1}$) states. However, the Xe(5d) states have much longer lifetimes (∼3 μs)[13a] and collisional relaxation as well as radiative decay to Xe(6p) levels must be evaluated. Two equivalent possibilities exist for generation of the Xe(6s[3/2]$_1$) emission: (i) The initially formed Xe(5d[7/2]$_3$ and [3/2]$_2$) atoms collide with Kr and form metastable Kr(5s[3/2]$_2$) atoms, which subsequently collide with Xe and transfer the excitation back to the Xe(6p) states.[7b,c] (ii) Another possibility is collisions of the Xe(5d) states with Xe or Kr with intermultiplet relaxation

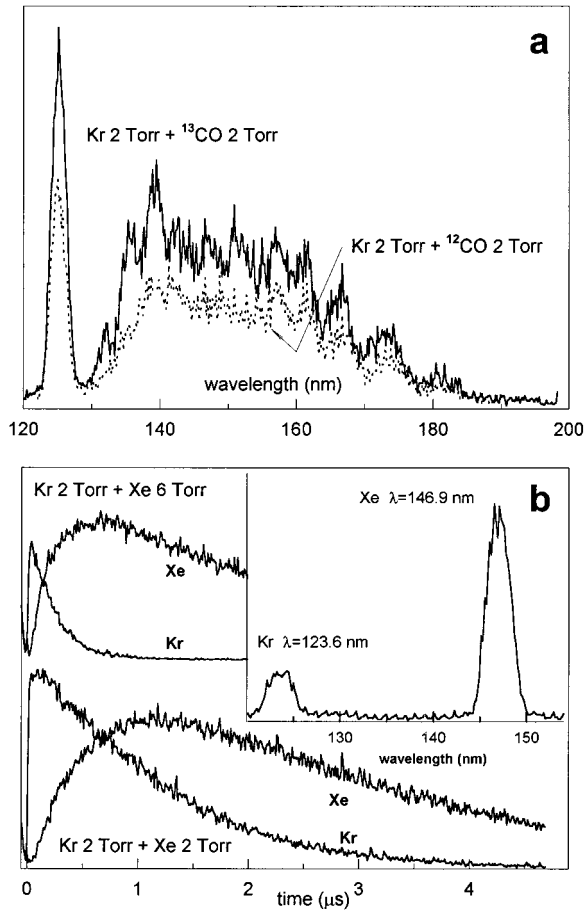

Figure 5. (a) Emission spectra from reactions of ^{12}CO and ^{13}CO with the Kr(5s[3/2]$_1$) resonance atoms. The emission in the λ > 130 nm range is the CO($A^1\Pi \rightarrow X^1\Sigma^+$) transition. The CO ($A^1\Pi$) state is formed by energy transfer from Kr(5s[3/2]$_1$) atoms as deduced from comparison of decay profiles (not shown here) for the (CO($A^1\Pi \rightarrow X^1\Sigma^+$) and Kr(5s[3/2]$_1 \rightarrow {}^1S_0$) emission intensities. (b) Decay profiles of Kr resonance emission at 123.6 nm and Xe resonance emission at 146.9 nm obtained under two-photon ASE generation of the Kr(5s[3/2]$_1$) state. The insert displays an emission spectrum from a mixture consisting of 2 Torr of Kr and 6 Torr of Xe.

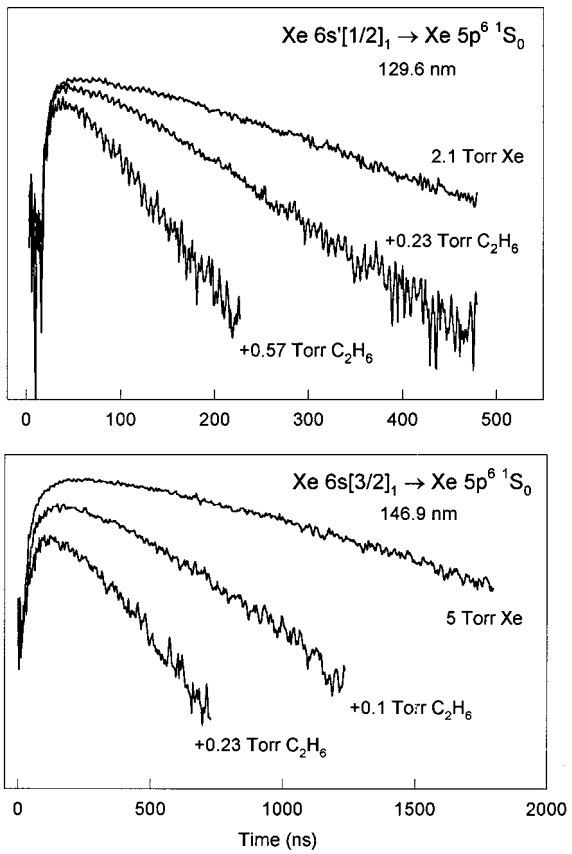

Figure 6. Decay profiles on a logarithmic scale of Xe(6s) and Xe(6s′) resonance fluorescence following excitation of Xe(6p′[3/2]$_2$) at 224.3 nm in a Xe/C_2H_6 mixture. Note the different scales for the two time axes.

to Xe(6p[1/2]$_0$). The quenching rate of this state by Xe is very slow, and collisions with Kr mainly gives metastable Kr(5s[3/2]$_2$), which subsequently transfers the energy back to Xe(6p) levels in collisions with Xe.[7] Thus, the absence of emission from Xe(5d[1/2]$_1$) at 125 nm and Xe(6s′[1/2]$_1$) at 129 nm can be explained. Although the evidence is indirect, quenching of Kr(5s[3/2]$_1$) probably gives mainly Xe(5d[7/2]$_3$ and 5d[3/2]$_2$) states as products. Interpretation of the failure to observe the 125 mm emission must be done with caution because radiation trapping may result in the 5d[1/2]$_1 \rightarrow$ 6p + $h\nu$ radiative pathway becoming favored.[13c] In contrast with the 5s[3/2]$_1$ atoms, the metastable Kr(5s[3/2]$_2$) + Xe reaction gives mainly Xe(6p[3/2]$_{1,2}$) products with only 10−15% formation of Xe(5d[1/2]$_1$ and 5d[1/2]$_0$),[6b,24] even though the energy is nearly resonant with the 5d[1/2]$_1$ state.

Previous experiments[6a,9] have shown that the Kr resonance and metastable state atoms both undergo similar reactive quenching with halogen containing polyatomic molecules such as CCl_4, CF_3Cl, and CF_3Br, although the yields of KrX(X=Cl,Br) are lower than for corresponding reactions with Xe(6s[3/2]$_{1,2}$) atoms. Golde's systematic study[11] of the products from Ar and Kr metastable atom reactions with many polyatomic molecules demonstrated that the most likely products from the hydrocarbon reagents in the bottom half of Table 1 arise from excitation transfer followed by dissociation involving the breaking of single bonds to give one or more atoms and a polyatomic radical. The reaction of resonance Kr atoms with H_2O and the 123.6 nm photolysis of H_2O gives OH($A^2\Sigma^+$,v'=0) with similar inverted rotational distributions.[22c] The Kr(5s[3/2]$_2$) metastable atom reaction with H_2O under thermal conditions does not give OH(A) as a product; however, the 5s′[1/2]$_0$ metastable atom reaction does give strong OH(A) emission.[6a,23] Interpretation of results from experiments[22d] that have both Kr metastable states present must be done carefully. Comparison of the OH(A,v',J') distributions from photolysis at 116.5 nm and the reactions of Kr(5s′[1/2]$_{1,0}$) atoms could be a useful test for interaction mechanisms.

D. Quenching Rate Constants for Xe(6s[3/2]$_1$) and Xe(6s′[1/2]$_1$) Atoms. In order to facilitate comparison of rate constants for the Kr and Xe resonance state atoms for a common set of reagents, a few additional rate constants were measured for Xe(6s[3/2]$_1$) and Xe(6s′[1/2]$_1$) atoms using a variation of the two-photon method described in earlier work.[1] In the present experiments, two-photon excitation at 224.3 nm to Xe(6p′[3/2]$_2$) was used to simultaneously generate the Xe(6s′) and Xe(6s) resonance states. This method was chosen because the BBO-II doubling crystal and the same dye as used for the Kr(5s[3/2]$_1$) experiments could be employed. Examples of the decay profiles of the Xe(6s) and Xe(6s′) resonance fluorescence in Xe/C_2H_6 mixtures are shown in Figure 6. The rise time for the 129.6 nm fluorescence from Xe(6s′[1/2]$_1$) atoms is prompt, and the maximum fluorescence intensity is not affected by the addition of C_2H_6. Both observations are as expected from the ASE generation process. This is not the case for the 149 nm fluorescence. The rise time does not follow the laser pulse and

TABLE 2: Comparison of Quenching Rate Constants[a] for Xe[b,c] and Kr Resonance State Atoms

reagent	Xe(6s[3/2]$_1$) 8.44 eV	Xe(6s′[1/2]$_1$) 9.57 eV	Kr(5s[3/2]$_1$) 10.03 eV
NO[c]	30 (0.8)[e]	80 (2)[e]	24 (2)[e]
CO_2[c]	52 (0.7)	76 (0.8)	34 (0.2)
N_2O[c]	72 (8.7)	98 (100)	43 (6.1)
OCS[b]	81 (80)	79 (200)	53 (20)
SO_2[b]	48 (4.1)	99 (20)	74 (41)
C_2H_2[c]	75 (81)	120 (37)	46 (8.1)
C_2N_2[b]	38 (4.1)	130 (160)	94 (122)
CH_4[c]	33 (0.02)	100 (30)	75 (30)
CH_3F[c]	37 (0.4)	110 (12)	48 (8)
C_2H_6[b]	61 (4.0)	94 (48)	82 (40)
cyclo-C_3H_6[b]	51 (16)	85 (32)	69 (64)
H_2[d]	0.86[f]		1.6[f]
D_2[d]	0.47[f]		1.4[f]

[a] In units of 10^{-11} cm^{-3} molecule^{-1} s^{-1}. [b] These data for quenching of the Xe states were acquired in the present study; see text. [c] These rate constants for the Xe states were reported in ref 1. [d] These rate constants were reported in ref 27; the rate constants for metastable Xe are 1.64×10^{-11} and 1.12×10^{-11} cm^3 s^{-1} for H_2 and D_2, respectively. [e] Photoabsorption cross section in units of 10^{-18} cm^2 from ref 29; the entry for CH_3F was obtained by comparison of electron scattering cross sections given in ref 29b for CH_4 and CH_3F. [f] The absorption cross sections for H_2 and D_2 are zero.

the peak emission intensity is reduced by the added reagents. These observations show that the 6s[3/2]$_1$ atoms are formed by radiative cascade from precursor Xe* levels other than Xe(6p′[1/2]$_1$) and not mainly by ASE. The most likely precursors are populations in the Xe(6p) levels, which could arise from Xe(7s or 5d) states formed by ASE. The quenching rate constants for Xe(6p[3/2]$_1$) atoms still can be measured because radiation trapping extends the effective lifetime to well beyond the time during which the resonance atoms are formed.

The Xe(6s′) atoms decay more rapidly than the Xe(6s) atoms, because the rate-limiting process is collisional transfer to the Xe(6p[1/2]$_1$) level, which then radiatively decays to Xe(6s), rather than radiation trapping of the 129.6 nm resonance light. Since the decay time of Xe(6s′) atoms is shorter than for Xe(6s) atoms, separate experiments were done to obtain their rate constants because higher reagent pressures are required for the Xe(6s′) atoms. The molecules selected for study were OCS, SO_2, C_2N_2, C_2H_6, and cyclo-C_3H_6. The plots of decay constants vs reagent pressure were of similar quality to those of ref 1. The rate constants listed in Table 2 for the Xe(6s,6s′) resonance states should have uncertainties of ±5%.

Discussion

A. Generation of Kr(5s[3/2]$_1$) Atoms and Measurement of Quenching Rate Constants. Pulsed, two-photon laser excitation of Kr(5p[5/2]$_2$) atoms with concomitant ASE provides an excellent source for Kr(5s) resonance state atoms. Since the radiative lifetime is lengthened by radiation trapping, measurement of the decay times of the Kr(5s[3/2]$_1$) atoms in the presence of added reagent gases allows reliable rate constants to be obtained. Except for products with radiative lifetimes less than ~50 ns, the method is less useful for identification of primary product states since Kr pressures of ≥0.5 Torr are needed. Because of the more favorable wavelength range for our laser, we used Kr(5p[5/2]$_2$) as the upper state. However, the Kr(5p[1/2]$_0$) state (212.5 nm) could be employed, which would ensure that Kr(5s[3/2]$_1$) atoms were prepared in the total absence of Kr(5s[3/2]$_2$) metastable atoms; such experiments would be preferable for identification of product states. Extension of the ASE method to prepare and study the second resonance state, Kr(5s′[1/2]$_1$), would require laser excitation of Kr(5p′[3/2]$_2$) at 204.2 nm. In addition to measuring quenching rate constants, such experiments with Kr[5s′] atoms would enable tests to be made for the degree of conservation of the $Kr^+(^2P_{1/2})$ ion core in reactive quenching reactions with halogen-containing molecules (RX). Such results could be compared to the reactions of Kr(5s′[1/2]$_0$) metastable atoms, which exhibited a high degree of core conservation and an even stronger propensity against formation of krypton halide molecules in the KrX(C,Ω=$^3/_2$) state.[6a]

We measured quenching rate constants at room temperature for 30 reagents that were selected to have a range of molecular properties. The magnitudes of the rate constants increased from 0.66×10^{-11} cm^3 molecule^{-1} s^{-1} for CF_4 upward to 74×10^{-11} cm^3 molecule^{-1} s^{-1} for C_2N_2. As already mentioned, the statistical uncertainties of these measurements are thought to be ±5%. Several of our quenching constants can be compared to the set of relative rate constants reported by Yu and Wang.[20] They employed a microwave-driven Kr lamp as a 123.6 nm source and recorded the decline in the steady-state resonance fluorescence intensity vs added reagent pressure in sensitized experiments. By normalizing each Stern−Volmer plot to that from CO_2, rate constants relative to CO_2 were obtained for eight other gases. By using our value for k_{CO_2}, we can convert their relative rate constants to absolute values. The agreement between their rate constants and ours is very good for N_2, H_2, O_2, and C_2H_2. However, their values are about 2 times higher than ours for Xe, CO, and N_2O. Although we did not study Cl_2, their rate constant is suspiciously large. Since we have independent, duplicate data sets for CO and Xe, we are confident of our results. Furthermore, the rate constant reported by Cook and Leichner[12] for Xe, 2.97×10^{-11} cm^3 s^{-1}, agrees with our result. The degree of agreement of rate constants obtained from the steady-state and pulsed source of Kr(5s[3/2]$_1$) atoms resembles the situation for Xe(6s[3/2]$_1$)[25] in that a few of the rate constants measured by the steady-state method are anomalously large. Cook and Leichner[12] also reported a rate constant for quenching of Kr(5s′[1/2]$_1$) by Xe, which was 8 times smaller than for Kr(5s[3/2]$_1$).[12b] The quenching rate constant for Kr(5s′[1/2]$_0$) atoms[6b] is $(24.2 \pm 1.5) \times 10^{-11}$ cm^3 s^{-1}, and the Xe quenching rate constants of both metastable states are larger than for their corresponding resonance states. Not enough is known about the Kr(5s,5s′) + Xe entrance channel potentials[26] to explain the wide disparity among the Kr(5s[3/2]$_{2,1}$ and 5s′[1/2]$_{1,0}$) quenching constants by Xe.

B. Interpretation of the Quenching Cross Sections. Since theoretical models that describe the interaction between electronically excited atoms with 10 eV of energy and polyatomic molecules do not exist, we will utilize empirical comparisons and correlations. The rate constants for Kr(5s[3/2]$_1$) resonance state (10.03 eV) atoms can be compared to those for Xe(6p[3/2]$_2$) atoms with 9.82 eV of energy. The latter can be considered as representative for states in the Xe(6p) manifold. As shown in Table 1, the Xe(6p) rate constants are larger than for the Kr(6s) resonance state in every instance. With the exception of collisions with Xe and CF_4, the quenching mechanism for Xe(6p) atoms is excitation transfer and not intramultiplet relaxation.[7a] Even though the acceptor product states for a given reagent should be the same for the two reactions, the larger collision diameter, the larger polarizability and the greater coupling strengths of Xe(6p) atoms lead to larger rate constants (and average thermal cross sections). The *very* much larger cross sections for H_2, CO, and N_2 are especially noteworthy. One

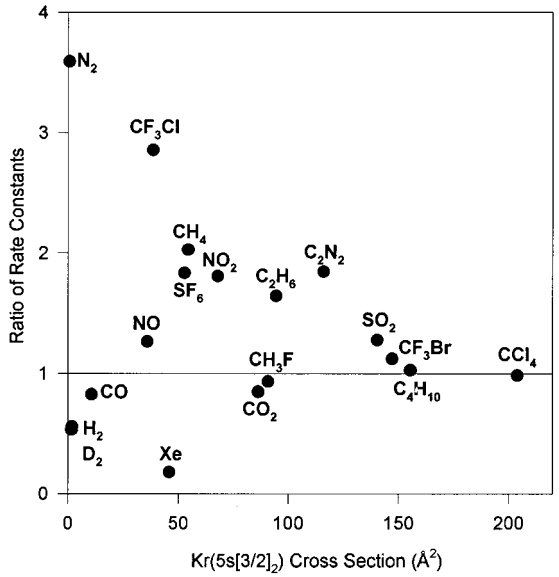

Figure 7. Comparison of the ratio of the quenching rate constants of Kr(5s[3/2]$_1$) to Kr(5s[3/2]$_2$) atoms for several reagents. The ratio is plotted vs the thermal quenching cross sections ($\sigma = k_Q/\langle V \rangle$) of the metastable atoms.

possible explanation is the more attractive interaction potentials for Xe(6p) than Kr(5s) because of contributions from Rydberg states built from the bound Xe^+-CO, Xe^+-N_2, and Xe^+-H_2 ion cores. Even the Xe(6s′) resonance state with 9.57 eV of energy generally has larger quenching constants than the Kr(5s) atoms, as illustrated by the data in Table 2. The comparison of Xe(6p) and Kr(5s) reactive cross sections for the same reagent clearly demonstrate that the nature of the excited state atom is important even for states of similar energy.

The ratio of quenching rate constants (or cross sections) for the resonance and metastable Kr(5s) atoms is plotted vs the cross section of the metastable atom in Figure 7. The CF_4 data point has been excluded because the quenching mechanism is intramultiplet relaxation. The ratio is $\sim>1$ for all molecules with the exception of $H_2(D_2)$. The general trend is for the ratio to become closer to unity for increasing total cross sections; i.e., the cross sections for both states approach the same orbiting limit. The average ratio of the quenching cross section for the molecules in Figure 7 with metastable cross sections larger than 5 Å^2 is 1.45; the average ratio declines to 1.36 for those reagents with metastable cross sections larger than 20 Å^2.

The data set for Xe(6s[3/2]$_1$) is limited to the rate constants of the molecules in Table 2 plus Cl_2, ClF, and CCl_4. As for Kr(5s) atoms, the ratio of resonance[27] to metastable rate constants is less than one for H_2 and (D_2). If H_2 and D_2 are excluded, the ratio of the resonance to metastable rate constants is 1.2. The largest ratio, $\sim$1.6, is for CO and N_2O. If they are excluded, the rate constants ratio drops to 1.1. The rate constants for a group of molecules similar to those in Table 2 can be compared for Ar(4s[3/2]$_1$) and Ar(4s[3/2]$_2$), although the data set for Ar(4s[3/2]$_1$) may have some limitations. For example, the more recent rate constant measurement[12a] for SF_6 (42×10^{-11} cm^3 s^{-1}) is 45% lower than the original report (see Table 2 in ref 8a for a summary of the older data). The Ar(4s[3/2]$_1$)/Ar(4s[3/2/]$_2$) rate constant ratios for hydrocarbon reagents are in the 0.85−0.95 range. Yoshida et al.[12b] recently made a comparison for CH_4, SiH_4, and GeH_4 using pulsed radiolysis and found an average ratio of 1.4. Within the experimental uncertainties, the rate constant ratio for the resonance and metastable atoms of Ar seem to be nearly unity. Yokayama and Hatano[28] have published a set of rate constants for the three Ne(3s[3/2]$_2$, [3/2]$_1$, [1/2]$_0$) states. The rate constants for the Ne(3s[3/2]$_1$) atoms are systematically larger than the mean value of the two metastable states. Considering all the rare gases, we can conclude that the quenching rate constants for the resonance state atoms are generally slightly larger than for metastable state atoms with the ratio becoming more nearly unity for the reactions with the larger rate constants.

The quenching cross sections for the first metastable states of Ar and Xe (and by implication Kr) by polyatomic molecules have been discussed[8b] in terms of long-range models, including the absorbing sphere and the classical orbiting limit; strong correlations do exist with the polarizability of the reagent and with the attractive well depth of the van der Waals potential of the collision pair. As the reagent molecules become more complex, the probability of quenching approaches unity in terms of these long-range models. Since the quenching cross sections of the resonance states have a nearly constant relation to the metastable states, it follows that the correlations just mentioned for the metastable states could be applied to the resonance states too. This brings us to an old, but still unresolved question. What is the contribution of the long-range, dipole−dipole mechanism to the quenching of the resonance states of the rare gas atoms? In our opinion, the dipole−dipole mechanism plays only a minor role. The major mechanism for quenching of the resonance, metastable and (n+1)p states of Ar, Kr, and Xe atoms is coupling of the entrance channel to excited electronic states of the polyatomic molecule by crossings (or avoided crossings) of the entrance and exit channel potentials. The large density of excited states ensures a high probability for quenching. We will support our opinion by three main arguments.

The best test for any quenching mechanism is identification of the primary products of the reaction. The most likely candidate for demonstration of a dipole−dipole component was the Kr(5s[3/2]$_1$) + CO reaction. However, comparison of ^{12}CO and ^{13}CO failed to show any major difference in either rate constant or product distribution, even though only ^{13}CO is expected to have a dipole−dipole component. The large quenching constants and the products of the Xe(6p) states also are not explained by the dipole−dipole model. The optically allowed transitions are between the Xe(6p−6s) levels with energies of $\sim$1.5 eV, and most molecules do not have available acceptor states in this energy range. The large cross sections result from excitation-transfer processes to acceptor states of the molecule corresponding to the Xe(6p) energy. The general similarity of products for metastable and resonance state atoms reactions is not consistent with the dipole−dipole mechanism, because the theory formally cannot hold for $J = 2$ or 0 atomic states that have singlet, $J = 0$, ground states. Except for a very small number of fortuitous cases and possibly the augmentation of cross sections for a few other cases, the product state information does not support the general importance of a dipole−dipole mechanism.

As shown in Figure 7, the quenching cross sections of the Kr resonance state are somewhat larger than for the metastable state and a similar trend exists for Xe. One might claim that this difference is just the contribution of the dipole−dipole mechanism to the enhanced quenching for the $J = 1$ state. However, the same trend exists for the Ne states, and the oscillator strength for Ne(3s′[1/2]$_1$) is too small to support a dipole−dipole mechanism.[28] Thus, this trend is not necessarily indicative of a dipole−dipole contribution. The general correspondence between the chemistry of the metastable and

resonance states is the strongest evidence against the dipole−dipole model for quenching of the rare gas atom resonance states.

The main evidence in support of a dipole−dipole mechanism for quenching of resonance states has been the agreement with calculated cross sections for a selected set of reagents. The frequently used Watanabe−Katsuura formulation[30,12] is given by eq 4 with σ_Q in atomic units squared.

$$\sigma_Q = 13.88(\mu_{Kr}{}^2\mu_Q{}^2/\hbar v)^{2/5} \quad (4)$$

The μ_{Kr} and μ_Q terms are the dipole transition matrix elements of the Kr and molecular transitions at the energy of the atomic transition, respectively, and v is the relative velocity of the collision pair. The transition matrix elements can be calculated from the oscillator strengths and absorption coefficients.

$$\mu_{Kr}{}^2 = (R/E)f_{Kr}; \quad \mu^2{}_Q = (2R^2/4\pi^2\alpha a_0{}^2E)\sigma_{abs} \quad (5)$$

where R, α, a_0, E, and f_{Kr} are the Rydberg constant, the fine structure constant, the Bohr radius, the energy of the resonance state, the oscillator strength of the resonance state, and the photoabsorption cross section of the molecule, respectively. The molecules selected for study in Table 1 actually were chosen, in part, to scan a wide range of σ_{abs} without having the complication of a reactive quenching exit channel giving XeO* or XeX* (X = halogen) as products. Comparison of the experimental and calculated cross sections of Kr(5s[3/2]$_1$) is given in Figure 8a for thermal velocity collisions of the molecules listed in Table 2 plus C_2H_4, C_3H_8 and C_4H_{10} from Table 1. As sometimes is the case, a moderately good correlation does exist, although the calculated value for CO_2 is too small and those for C_3H_6 and C_2N_2 are too large. Other examples could be selected from Table 1 for comparison; the rate constants for NO and O_2 are nearly equal, but the absorption coefficient differ by a factor of 13. The $\sigma_Q{}^{2/5}$ dependence makes the test rather insensitive to small changes in σ_{abs}.

A more rigorous test is to examine the quenching cross sections for the three resonance states of Kr and Xe. Since we know the oscillator strengths of the three states, this comparison can be made on the same type of plot. The contributions of the atomic parts to eq 4 are in the relative order 1.0, 0.88, and 0.77 for Xe(6s), Xe(6s′), and Kr(5s), respectively. These ratios are also approximately equivalent to the ratio of the Lennard-Jones collision diameters. Since the contributions from the atoms to eq 5 are nearly equal, the variation of the quenching cross sections in this series will mainly depend on σ_{abs} of the molecule. The plots in Figure 8, b and c, show that the overall agreement is much poorer for the Xe* states than for Kr*; the correspondence between the calculated and experimental cross sections is especially poor for Xe(6s′). In fact, the Xe(6s′) cross sections tend to cluster around 200 Å^2 and have a weak dependence on σ_{abs}. The most serious discrepancies for the set of Xe(6s) rate constants are CH_4, CH_3F, CO_2, C_2H_2, and COS. Methane was chosen precisely because of its very small σ_{abs} value at 147 nm; the calculated cross section for Xe(6s) is too small by a factor of 2; however, the calculated values for CH_4 do match the data for Kr(5s) and Xe(6s′). The calculated values for CO_2 are too small for all three atoms by a factor of ∼3. The large σ_{abs} of OCS and C_2H_2 are not matched by corresponding large quenching cross sections for Xe(6s). The discrepancy for OCS is even greater for Xe(6s′); however, the calculation quenching cross section for Kr(5s) became close to the experimental value because σ_{obs} becomes smaller at 123.6 nm. Another test molecule was N_2O; the quenching cross sections do scale with σ_{abs}, but the calculated value is 50% too large for Xe(6s′). We reach the conclusion that the agreement between experimental and calculated dipole−dipole cross sections is qualitative. The general scaling of cross sections with σ_{abs} is a consequence of the fact that σ_{abs} is an index of the number of available acceptor states for coupling to the entrance channel potential. It should be noted that other types of quenching models[8a] also utilize the two-fifths power dependence of the photoabsorption cross sections as a measure of suitable acceptor states. Golde has used the product of the $N_2(A-X,v'')$ Franck−Condon factors and absorption cross sections of the reagent to successfully correlate the quenching rate constants of metastable $N_2(A^3\Sigma^+_u)$ molecules.[31]

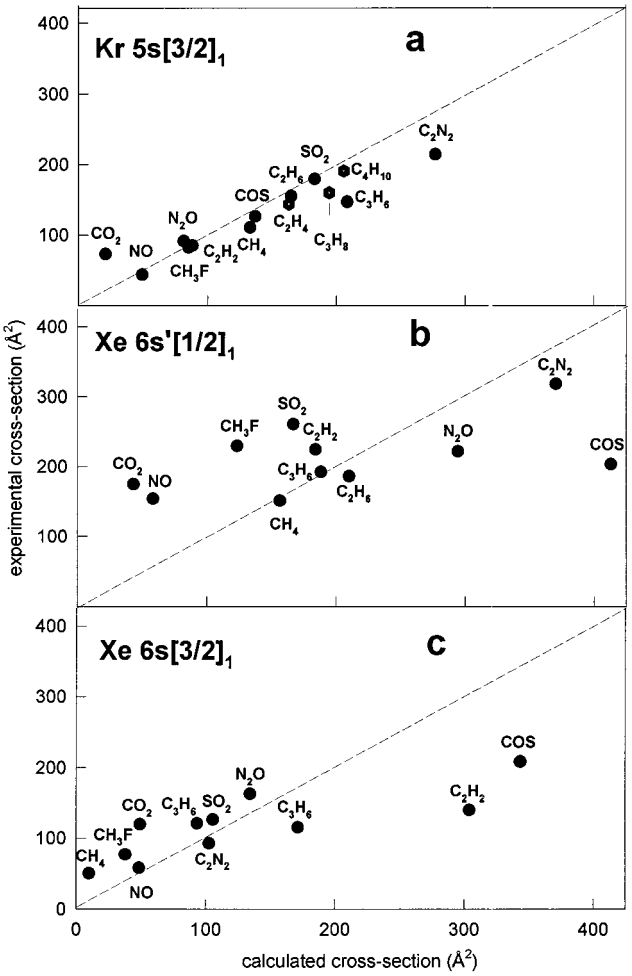

Figure 8. Comparison of experimental quenching cross sections for the set of 11 reagents in Table 2 with the theoretical cross sections calculated from the dipole−dipole model for Kr and Xe resonance states: (a) Kr(5s[3/1]$_1$), (b) Xe(6s′[1/2]$_1$); (c) Xe(6s[3/2]$_1$). Three additional points (C_4H_{10}, C_3H_8, and C_2H_4) are shown for Kr(5s) atoms.

Conclusions

The two-photon pulsed laser excitation of Kr(5p[5/2]$_2$) with concomitant ASE was used to generate the Kr[5s[3/2]$_1$) resonance state atoms in a few Torr of Kr. Room temperature quenching rate constants were measured for 30 reagent gases. The method is demonstrated to be highly reliable, and the quenching constants have an uncertainty of ±5%. In addition to the Kr(5s[3/2)$_1$) measurements, experiments were done to measure some additional quenching rate constants for Xe(6s-[3/2]$_1$) and Xe(6s′[1/2]$_1$) resonance state atoms. Comparison of quenching cross sections for the three resonance states for a set

of 11 common reagent molecules was done to test the validity of the dipole−dipole quenching model. Although the agreement between the calculated and experimental quenching cross sections is encouraging for Kr(5s[3/2]$_1$) atoms, the fits are poor for the Xe(6s) and Xe(6s′) resonance atoms. As for many other long-range quenching models, the photoabsorption cross section scales with other molecular properties that correlate with quenching cross sections. However, quantitative agreement with the dipole−dipole model is lacking when a range of molecules is examined for all three resonance atoms. In general, the quenching cross sections are slightly larger for the Xe(6s) and Kr(5s) resonance states than for their corresponding metastable states. However, the difference becomes much smaller as the quenching cross sections become larger, and both approach the same upper limit.

Acknowledgment. This work was supported by the U.S. National Science Foundation, CHE-9505032. We thank Dr. Wayne Danen of Los Alamos National Laboratory for arranging the loan of the vacuum UV monochromator which made this work possible.

References and Notes

(1) Alekseev, V. A.; Setser, D. W. *J. Chem. Phys.* **1996**, *105*, 4613.

(2) Alekseev, V. A.; Setser, D. W. *J. Phys. Chem.* **1996**, *100*, 5766.

(3) (a) Miller, J. C. *Phys. Rev. A* **1989**, *40*, 6969. (b) Rankin, M. B.; Davis, J. P.; Giranda, C.; Bobb, L. C. *Opt. Commun.* **1989**, *70*, 345.

(4) (a) Hamadani, S. M.; Stockdale, J. A. D.; Compton R. N.; Pindzola, M. S. *Phys. Rev.* **1986**, *A34*, 1938. (b) Malcuit, M. S.; Gauthier D. J.; Boyd, R. W. *Phys. Rev. Lett.* **1985**, *55*, 1086. (c) Boyd, R. W.; Malcuit, M. S.; Gauthier, D. J.; Rzazewski, K. *Phys. Rev.* **1987**, *A35*, 1648.

(5) Riley, M. E. *Phys. Rev.* **1990**, *A41*, 4843.

(6) (a) Zhong, D.-P.; Setser, D. W.; Sobczynski, R.; Gadomski, W. *J. Chem. Phys.* **1997**, *105*, 5020. (b) Sobczynski, R.; Setser, D. W. *J. Chem. Phys.* **1991**, *95*, 3310.

(7) (a) Nelson, T. O.; Setser, D. W.; Richmann, M. *J. Phys. Chem.* **1995**, *99*, 7482. (b) Xu, J.; Setser, D. W. *J. Chem. Phys.* **1990**, *92*, 4191. (c) Whitehead, C. A.; Pournasr, H.; Bruce, M. R.; Cai, H.; Kohel, J.; Layne, J. B.; Keto, J. *J. Chem. Phys.* **1995**, *102*, 1965.

(8) (a) Velazco, J. E.; Kolts. J. H.; Setser, D. W. *J. Chem. Phys.* **1978**, *69*, 4357, *71*, 1247. (b) Chen, X.; Setser, D. W. *J. Phys. Chem.* **1991**, *95*, 8473.

(9) (a) Brashers, H. C.; Setser, D. W. *J. Phys. Chem.* **1980**, *84*, 224. (b) Brashers, H. C.; Setser, D. W.; Yu, Y. C. *J. Phys. Chem.* **1980**, *84*, 2495; *J. Chem. Phys.* **1981**, *74*, 10. (c) Yu. Y. C.; Setser, D. W. *J. Phys. Chem.* **1990**, *94*, 2934.

(10) Sadeghi, N.; Cheaib, M.; Setser, D. W. *J. Chem. Phys.* **1989**, *90*, 219.

(11) (a) Balamuta, J.; Golde, M. F.; Ho, Y.-S. *J. Chem. Phys.* **1983**, *79*, 2822. (b) Balamuta J.; Golde, M. F. *J. Chem. Phys.* **1982**, *76*, 2430. (c) Balamuta, J.; Golde, M. F.; Moyle, A. M. *J. Chem. Phys.* **1985**, *82*, 3169. (d) Golde, M. F.; Ho, Y.-S. *J. Chem. Phys.* **1985**, *82*, 3160.

(12) (a) Ukai, M.; Koizumi, H.; Shinsaka, K.; Hatano, Y. *J. Chem. Phys.* **1986**, *84*, 3199. (b) Yoshida, H.; Kawamura, H.; Ukai, M.; Kouchi, N.; Hatano, Y. *J. Chem. Phys.* **1992**, *96*, 4372.

(13) (a) Aymar, M.; Coulomb, M. *At. Data Nucl. Data Tables* **1978**, *21*, 538. (b) Horiguchi, H.; Chang, R. S. F.; Setser, D. W. *J. Chem. Phys.* **1981**, *73* 1207. (c) Alekseev, V. A.; Setser, D. W. *J. Phys. Chem.*, submitted for publication.

(14) Matthias, E.; Rosenberg, R. A.; Poliakoff, E. D.; White, M. G.; Lee, S. T.; Shirley, D. A. *Chem. Phys. Lett.* **1977**, *52*, 239.

(15) Holstein, T. *Phys. Rev.* **1947**, *72*, 1212; **1951**, *83*, 1159.

(16) (a) Lawler, J. E.; Curry, J. U. *J. Phys. D.* **1998**, *31*, 1. (b) Hurst, G. S.; Wagner, E. B.; Payne, M. G. *J. Chem. Phys.* **1974**, *61*, 3680.

(17) (a) Audouard, E.; Laporle, P.; Suibtil, J. C.; Damany, N. *J. Chem. Phys.* **1998**, *89*, 6176. (b) Cook, J. D.; Leichner, P. K. *Phys. Rev. D* **1985**, *31*, 90. (c) Tracy, C. J.; Oskam, H. J. *J. Chem. Phys.* **1976**, *65*, 1666.

(18) Nelson, T. O.; Setser D. W. *Chem. Phys. Lett.* **1990**, *170*, 430.

(19) (a) Francis, A.; Czarnetzki, U.; Dobele, H. F.; Sadeghi, N. *Appl. Phys. Lett.* **1997**, *71*, 3796. (b) Sadeghi, N. Private communication, 1998.

(20) Yu, Y. C.; Wang, K. J. *J. Photochem. Photobiol. A: Chem.* **1993**, *72*, 109.

(21) Sadeghi. N.; Columb, I.; Stoyanova, J.; Setser D. W.; Zhong, D. *J. Chem. Phys.* **1995**, *10*, 2244.

(22) (a) Vikis, A. C. *Chem. Phys. Lett.* **1978**, *57*, 522. (b) Vikis, A. C. *J. Chem. Phys.* **1978**, *69*, 697. (c) Vikis, A. C. *J. Chem. Phys.* **1978**, *68*, 4314. (d) Tabayashi, K.; Shobatake, K. *J. Chem. Phys.* **1988**, *88*, 835.

(23) (a) Sadeghi, N.; Setser, D. W. *Chem. Phys. Lett.* **1991**, *82*, 44. (b) Tsuji, M.; Yamaguchi, K.; Nishimura, Y. J. *Chem. Phys.* **1988**, *89*, 3391.

(24) Rickey, D.; Krenos, J. *J. Chem. Phys.* **1997**, *107*, 3135.

(25) Yu, Y. C. *J. Photochem. Photobiol. A: Chem.* **1989**, *47*, 259.

(26) (a) Lipson, R. H.; Dimov, S. S.; Hu, X. K.; Mao, D. M.; Cai, J. Y. *J. Chem. Phys.* **1995**, *103*, 6313. (b) Balakrishnan, A.; Jones, W. J.; Mahajah, C. G.; Stoicheff, B. P. *Chem. Phys. Lett.* **1989**, *155*, 43.

(27) Kanaev, A. V.; Moller, T.; Gurtler, P. *Chem. Phys. Lett.* **1992**, *198*, 157.

(28) Yokoyama, A.; Hatano, Y. *Chem. Phys.* **1981**, *63*, 59.

(29) (a) Okabe, H. *Photochemistry of Small Molecules*; Wiley: New York, 1978. (b) Robin, M. *High Excited States of Molecules*; Academic Press: New York, 1974.

(30) Watanabe, T.; Katsuura, K. J. *Chem. Phys.* **1967**, *47*, 800.

(31) Golde, M. F. *Int. J. Chem. Kinet.* **1988**, *20*, 75.